Electronic Supporting Information

Conversion of dinitrogen to tris(trimethylsilyl)amine catalyzed by titanium triamido-amine complexes

Priyabrata Ghana, Franziska D. van Krüchten, Thomas P. Spaniol, Jan van Leusen, Paul Kögerler, and Jun Okuda*

Institute of Inorganic Chemistry, RWTH Aachen University, Landoltweg 1, 52074 Aachen, Germany

Table of Contents

1. Experimental Section-General Part

All manipulations were performed under argon or N_2 atmosphere using standard Schlenk or glove box techniques. Prior to use, glassware was dried overnight at 150 °C and solvents were dried, distilled and degassed using standard methods. If not otherwise stated, the reactions were performed at room temperature (21-24 °C) in Schlenk flasks or Schlenk tubes of suitable size equipped with a PTFE magnetic stir bar. NMR measurements were performed on a Bruker DRX 400 at 24 °C at 400 MHz for ^1H nuclei, 40.57 MHz for ^{15}N nuclei, 79.5 MHz for ^{29}Si nuclei and 101 MHz for ^{13}C nuclei. The chemical shifts (δ in ppm) in the ^1H and $^{13}C\{^1H\}$ NMR spectra were referenced to the residual proton signals of the deuterated solvents and reported relative to tetramethylsilane. The chemical shifts in the ^{15}N and ^{29}Si NMR were referenced with respect to ammonia (δ = 0) and tetramethylsilane (δ = 0), respectively. If not otherwise stated, the signals in $^{13}C\{^1H\}$ NMR spectra are sharp singlets. Standard abbreviations indicating multiplicities were used as follows: s (singlet), d (doublet), t (triplet), m (multiplet). IR spectra were recorded using KBr pellets using an AVATAR 360 FT-IR spectrometer. The Raman spectra of solids filled in 2 mm vacuum sealed capillaries were recorded at room temperature on a Bruker MultiRam Ramanspectrometer (λ = 1064 nm, 5 mW; Nd:YAG laser, germanium detector). Elemental analyses were carried out using a CHN-O-Rapid VarioEL from Heraeus. Elemental analysis was performed using an *elementar vario EL* machine. GC MS spectra were recorded on a *Shimadzu GCMS-QP2010 Plus* machine. Helium was used as the carrier gas at 100 kPa. The column used was a *TG-5SIL MS* with 20m length. The method used was as follows: initial oven temperature 61 °C; initial hold time 2.1 min; rate 10 °C/min; final oven temperature 250°C; final hold time 4.2 min.

The starting materials $H_3(Xy-N_3N)$ $(Xy-N_3N = \{(3,5-Me_2C_6H_3)NCH_2CH_2\}_3N^{3-})$,[S1] $Ti(NMe_2)_4$,[S2] $LiCH_2SiMe_3$,[S3] and KC_8[S4] were prepared according to the reported procedures. [NEt$_3$H]Cl, 3M MeMgCl solution in THF, Li granular and naphthalene were purchased from Sigma Aldrich and used as received. Na and K were purchased from Sigma Aldrich and washed several times with *n*-pentane before use. $PhSiH_3$ was purchased from TCI chemicals.

2. Syntheses, spectroscopic data, and illustrations of the NMR spectra of all reported compounds

2.1. [Ti(NMe₂)(Xy-N₃N)] (1-NMe₂)

A yellow solution of H_3(Xy-N_3N) (2.52 g, 5.49 mmol) and [Ti(NMe$_2$)$_4$] (2.46 mL, 2.33 g, 10.39 mmol, 1.89 equiv.) in 200 mL of toluene was heated to 80 °C for 20 h under static vaccum. Upon heating the color of the solution changed to dark red. A ^{1}H NMR spectrum of an aliquot of the red solution after 20 h confirmed the completion of the reaction. The dark red solution was concentrated to ~20 mL and filtered to another Schlenk tube. The filtarate was treated with ~ 40 mL of *n*-pentane and stored at −40 °C for 15 h. Resulting precipitate was isolated as a bright red solid by filtration of the light red supernatant, washing with 4 mL of *n*-pentane at −40 °C and drying under reduced pressure for 2 h at ambient temperature; yield: 2.982 g (5.45 mmol, 99%). Elemental analysis calcd. (%) for $C_{32}H_{45}N_5Ti$ (547.6 g/mol): C 70.19, H 8.28, N 12.79%; found: C 69.53, H 8.22, N 12.75.

^{1}H NMR (400 MHz, benzene-d_6, 296 K): δ (ppm) = 2.28 (s, 18H, $C_6H_3(CH_3)_2$), 2.62 (s, 6H, N(CH_3)$_2$), 2.67 (t, ^3J(H,H) = 5.9 Hz, 6H, NCH_2), 3.69 (t, ^3J(H,H) = 5.9 Hz, 6H, N(Xy)CH_2), 6.57 (br s, 3H, C^4-H, C_6H_3), 6.82 (br s, 6H, $C^{2,6}$-H, C_6H_3).

^{13}C{^{1}H} NMR (101 MHz, benzene-d_6, 296 K): δ (ppm) = 21.7 (s, $C_6H_3(CH_3)_2$), 43.3 (s, N(CH_3)$_2$), 54.0 (s, NCH_2), 55.0 (s, N(Xy)CH_2), 119.0 (s, *o*-C_6H_3), 122.4 (s, *p*-C_6H_3), 137.3 (s, *m*-C_6H_3), 157.3 (s, *ipso*-C_6H_3).
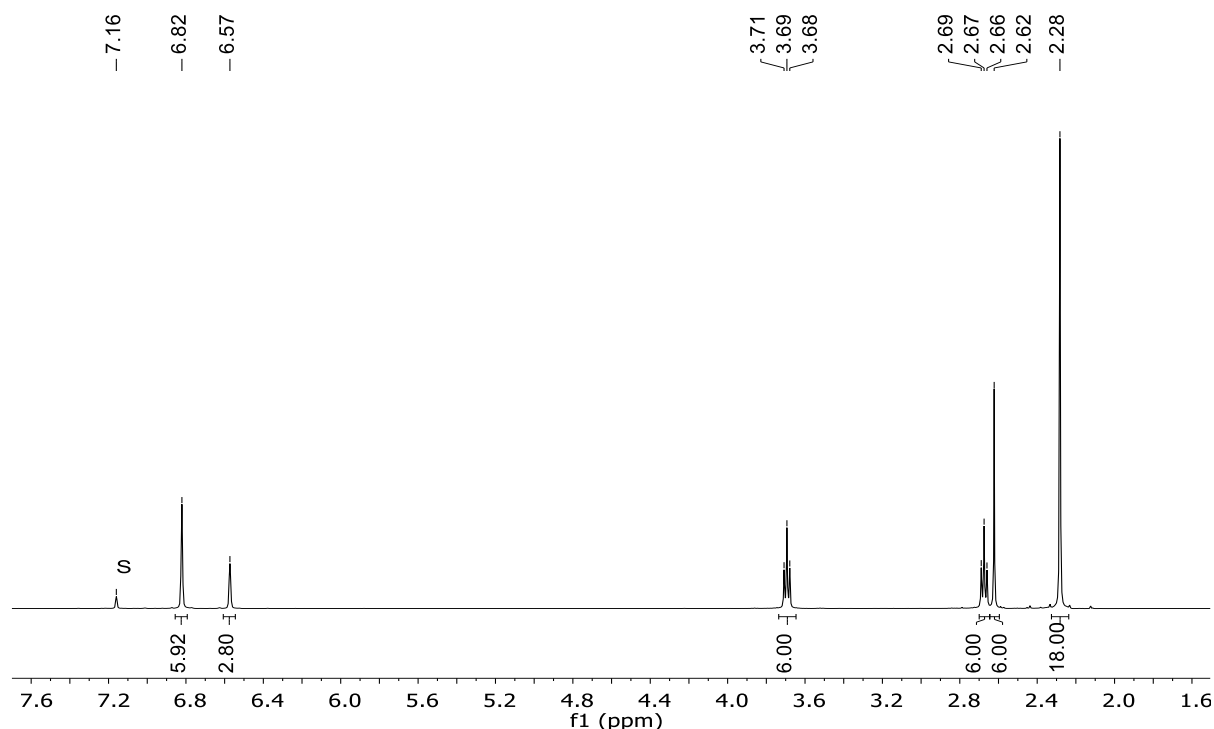
Figure S1. ^{1}H NMR spectrum of **1-NMe₂** in benzene-d_6 at 296 K; S denotes the residual proton signal of the deuterated solvent.
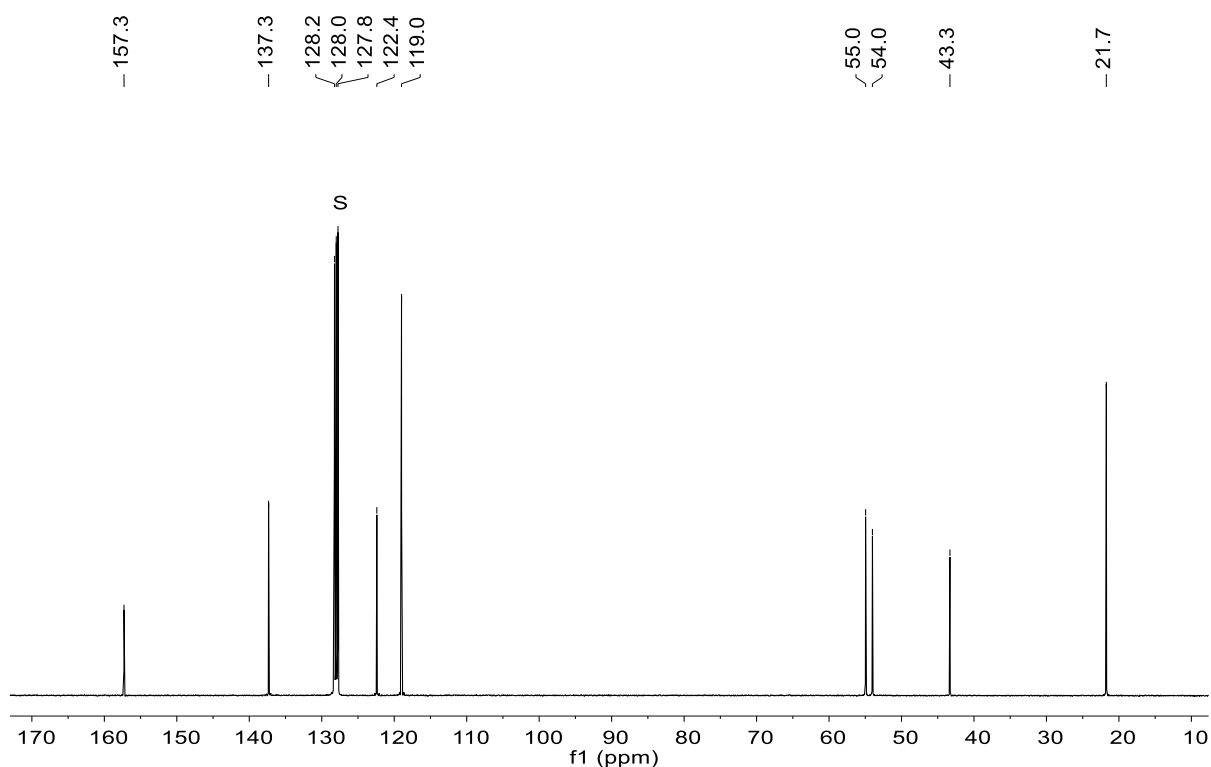
Figure S2. $^{13}C\{^1H\}$ NMR spectrum of **1-NMe₂** in benzene-d_6 at 296 K; S denotes the residual proton signal of the deuterated solvent.

2.2. [TiCl(Xy-N₃N)] (1-Cl)

A solid mixture of **1-NMe₂** (2.0 g, 3.65 mmol) and [NEt₃H]Cl (0.503 g, 3.65 mmol, 1 equiv.) was treated with ~100 mL of CH_2Cl_2 at ambient temperature and stirred for 2 h. Immediate after addition the color of the solution turn dark brown. A ^1H NMR spectrum of an aliquot of the reaction mixture after 2 h confirmed the completion of the reaction. All volatiles were removed under reduced pressure and the dark brown residue was washed with 30 mL of *n*-pentane at ambient temperature. Crystallization of the solid from a 3:1 mixture of *n*-pentane/CH_2Cl_2 (~60 mL) at −40 °C resulted in an analytically pure, dark brown, microcrystalline solid; Yield: 1.615 g (3.0 mmol, 82%). Elemental analysis calcd. (%) for $C_{30}H_{39}ClN_4Ti$ (539.0 g/mol): C 66.85, H 7.29, N 10.40%; found: C 65.99, H 7.56, N 10.51.

^1H NMR (400 MHz, benzene-d_6, 296 K): δ (ppm) = 2.22 (s, 18H, $C_6H_3(CH_3)_2$), 2.53 (t, ^3J(H,H) = 5.8 Hz, 6H, NCH_2), 3.68 (t, ^3J(H;H) = 5.8 Hz, 6H, NCH_2), 6.58 (br. s, 3H, *p*-C_6H_3), 6.95 (br. s, 6H, *o*-C_6H_3). ^1H NMR (400 MHz, THF-d_8, 296 K): δ (ppm) = 2.18 (s, 18H, $C_6H_3(CH_3)_2$), 3.34 (t, ^3J(H,H) = 5.8 Hz, 6H, NCH_2), 4.00 (t, ^3J(H;H) = 5.8 Hz, 6H, NCH_2), 6.48 (br. s, 3H, *p*-C_6H_3), 6.67 (br. s, 6H, *o*-C_6H_3).
$^{13}C\{^1H\}$ NMR (101 MHz, benzene-d_6, 296 K): δ (ppm) = 21.6 (s, $C_6H_3(CH_3)_2$), 55.6 (s, NCH_2), 56.1 (s, NCH_2), 119.2 (s, *o*-C_6H_3), 124.5 (s, *p*-C_6H_3), 137.6 (s, *m*-C_6H_3), 158.0 (s, *ipso*-C_6H_3).
$^{13}C\{^1H\}$ NMR (101 MHz, THF-d_8, 296 K): δ (ppm) = 21.7 (s, $C_6H_3(CH_3)_2$), 56.9 (s, NCH_2), 57.0 (s, NCH_2), 119.5 (s, *o*-C_6H_3), 124.2 (s, *p*-C_6H_3), 137.8 (s, *m*-C_6H_3), 158.0 (s, *ipso*-C_6H_3).
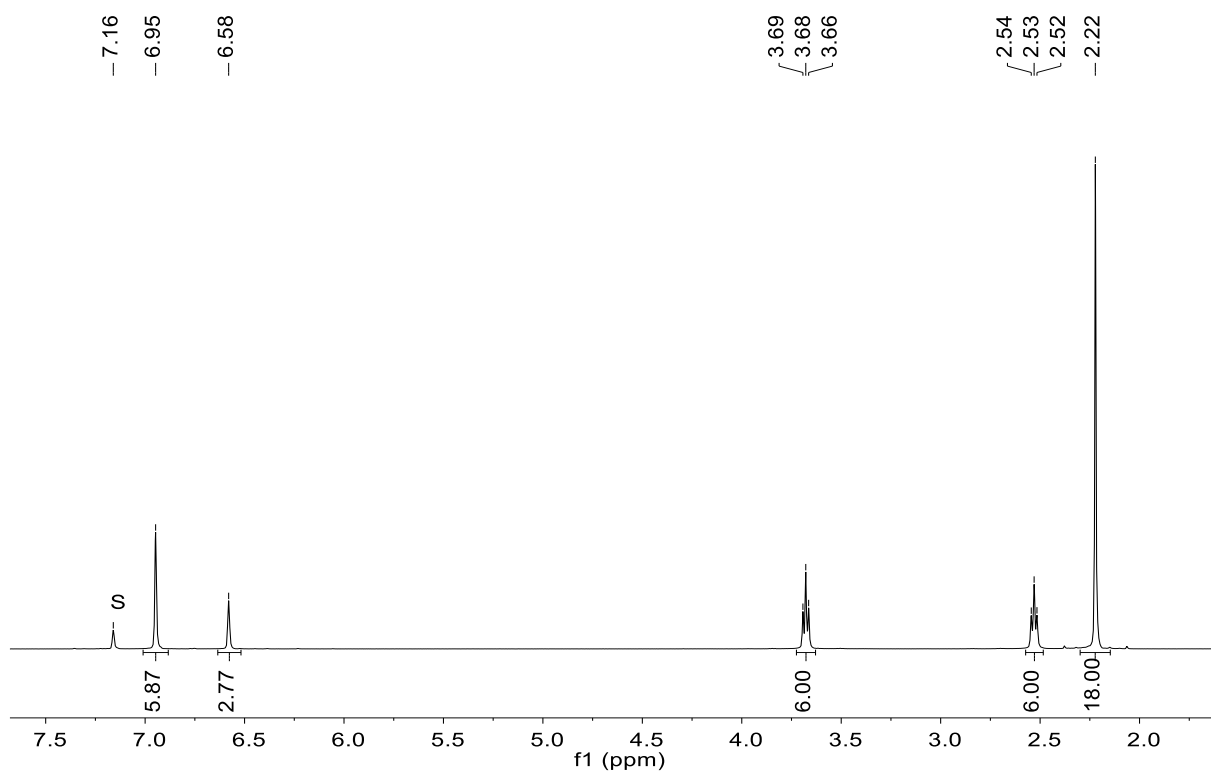
Figure S3. ^{1}H NMR spectrum of **1-Cl** in benzene-d_6 at 296 K; S denotes the residual proton signal of the deuterated solvent.
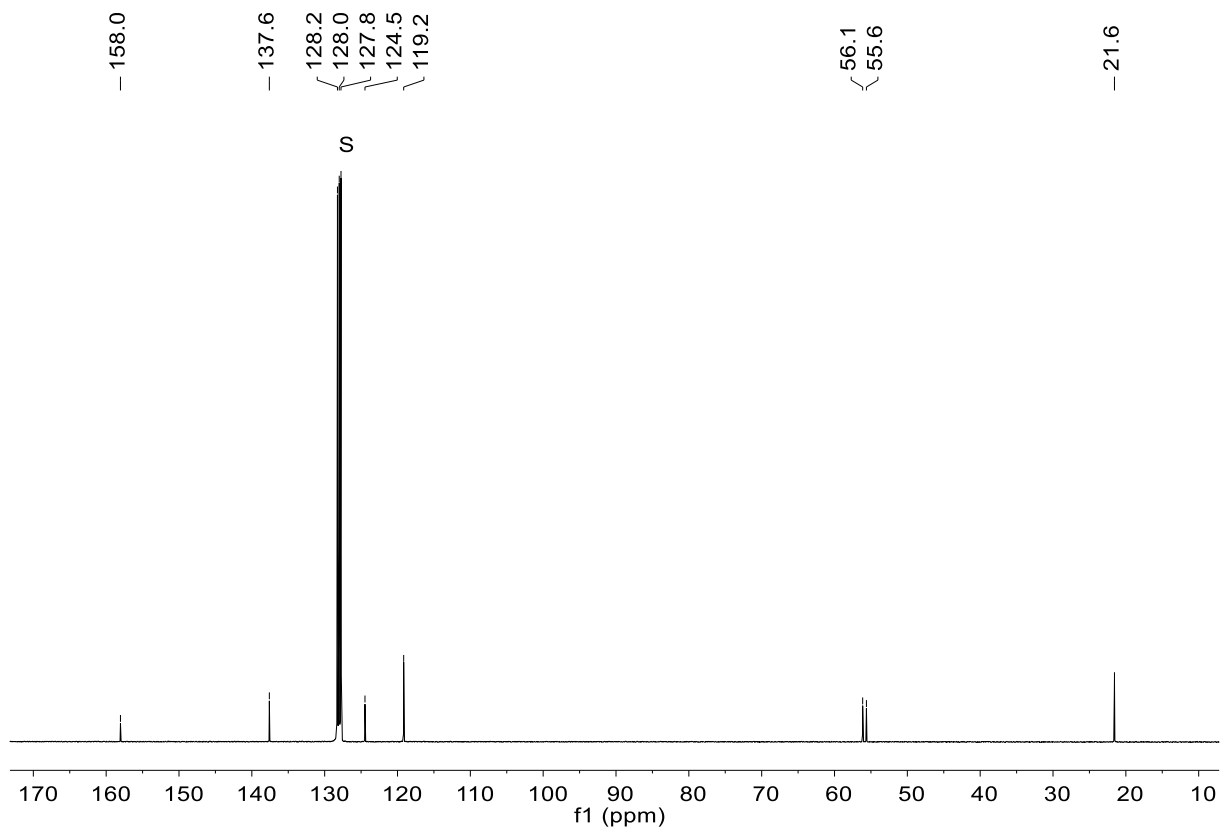
Figure S4. ^{13}C{^{1}H} NMR spectrum of **1-Cl** in benzene-d_6 at 296 K; S denotes the residual proton signal of the deuterated solvent.

2.3. [TiMe(Xy-N₃N)] (1-Me)

To a brown solution of **1-Cl** (200 mg, 0.37 mmol) in 15 mL of Et_2O, a 3 M solution of MeMgCl (148 μL, 0.44 mmol, 1.2 equiv.) in THF was added at −40 °C. The reaction mixture was stirred for 1 h at −40 °C and 1 h at room temperature resulting in a red suspension. The red suspension was treated with 10 μL of 1,4-dioxane at room temperature and stirred for another 1 h. The red suspension was filtered and the filtrate was evaporated to obtain a red powder; yield: 176 mg (0.34 mmol, 91%). Elemental analysis calcd. (%) for $C_{31}H_{42}N_4Ti$ (518.5 g/mol): C 71.80, H 8.16, N 10.80%; found: C 69.07, H 8.10, N 10.61.

^{1}H NMR (400 MHz, benzene-d_6, 296 K): δ (ppm) = 1.27 (s, 3H, TiCH_3), 2.24 (s, 18H, C_6H_3(CH_3)$_2$), 2.34 (t, ^3J(H,H) = 5.5 Hz, 6H, NCH_2), 3.63 (t, ^3J(H,H) = 5.5 Hz, 6H, NCH_2), 6.58 (br. s, 3H, p-C_6H_3), 6.93 (br. s, 3H, o-C_6H_3).

^{13}C{^{1}H} NMR (101 MHz, benzene-d_6, 296 K): δ (ppm) = 21.7 (s, C_6H_3(CH$_3$)$_2$), 54.7 (s, NCH$_2$), 55.1 (s, NCH$_2$), 71.4 (s, TiCH$_3$), 118.1 (s, o-C_6H_3), 123.4 (s, p-C_6H_3), 138.2 (s, m-C_6H_3), 156.2 (s, $ipso$-C_6H_3).

Figure S5. ^{1}H NMR spectrum of **1-Me** in benzene-d_6 at 296 K; S denotes the residual proton signal of the deuterated solvent.

Figure S6. $^{13}C\{^1H\}$ NMR spectrum of **1-Me** in benzene-d_6 at 296 K; S denotes the residual proton signal of the deuterated solvent.

2.4. [Ti(CH₂SiMe₃)(Xy-N₃N)] (1-CH₂SiMe₃)

A solid mixture of **1-Cl** (200 mg, 0.37 mmol) and LiCH₂SiMe₃ (38 mg, 0.40 mmol, 1.1 equiv.) was treated with 5 mL of diethylether at ambient temperature and the brown suspension was stirred for 3 h. All volatiles were removed under reduced pressure and the brown residue was extracted with 10 mL of *n*-pentane. Cooling of the extracts at −40 °C afforded brown needles, which were isolated by filtration of the supernatant; yield: 156 mg (0.26 mmol, 71% based on **1-Cl**). Elemental analysis calcd. (%) for $C_{34}H_{50}N_4SiTi$ (590.74 g/mol): C 69.13, H 8.53, N 9.48%; found: C 60.12, H 7.61, N 9.76.

^1H NMR (400 MHz, benzene-d_6, 296 K): δ (ppm) = −0.19 (s, 9H, Si(CH_3)₃), 2.30 (s, 18H, C₆H₃(CH_3)₂), 2.36 (s, 2H, SiCH_2), 2.38 (t, ^3J(H,H) = 5.8 Hz, 6H, NCH_2), 3.58 (t, ^3J(H,H) = 5.8 Hz, 6H, NCH_2), 6.61 (br s, 3H, *p*-C₆H_3), 6.98 (br s, 6H, *o*-C₆H_3).

^1H NMR (400 MHz, CD₂Cl₂, 296 K): δ (ppm) = −0.63 (s, 9H, Si(CH_3)₃), 1.83 (s, 2H, SiCH_2), 2.20 (s, 18H, C₆H₃(CH₃)₂), 3.14 (t, ^3J(H,H) = 5.8 Hz, 6H, NCH_2), 3.87 (t, ^3J(H,H) = 5.8 Hz, 6H, NCH_2), 6.50 (br s, 3H, *p*-C₆H_3), 6.68 (br s, 6H, *o*-C₆H_3).

$^{13}C\{^1H\}$ NMR (101 MHz, benzene-d_6, 296 K): δ (ppm) = 2.3 (s, Si(CH_3)₃), 21.7 (s, C₆H₃(CH_3)₂), 53.5 (s, NCH_2), 53.8 (s, NCH_2), 95.8 (s, SiCH_2), 117.3 (s, *o*-C₆H₃), 122.7 (s, *p*-C₆H₃), 138.1 (s, *m*-C₆H₃), 156.6 (s, *ipso*-C₆H₃).

$^{29}Si\{^1H\}$ NMR (79.5 MHz, benzene-d_6, 296 K): δ (ppm) = −4.45 ppm.
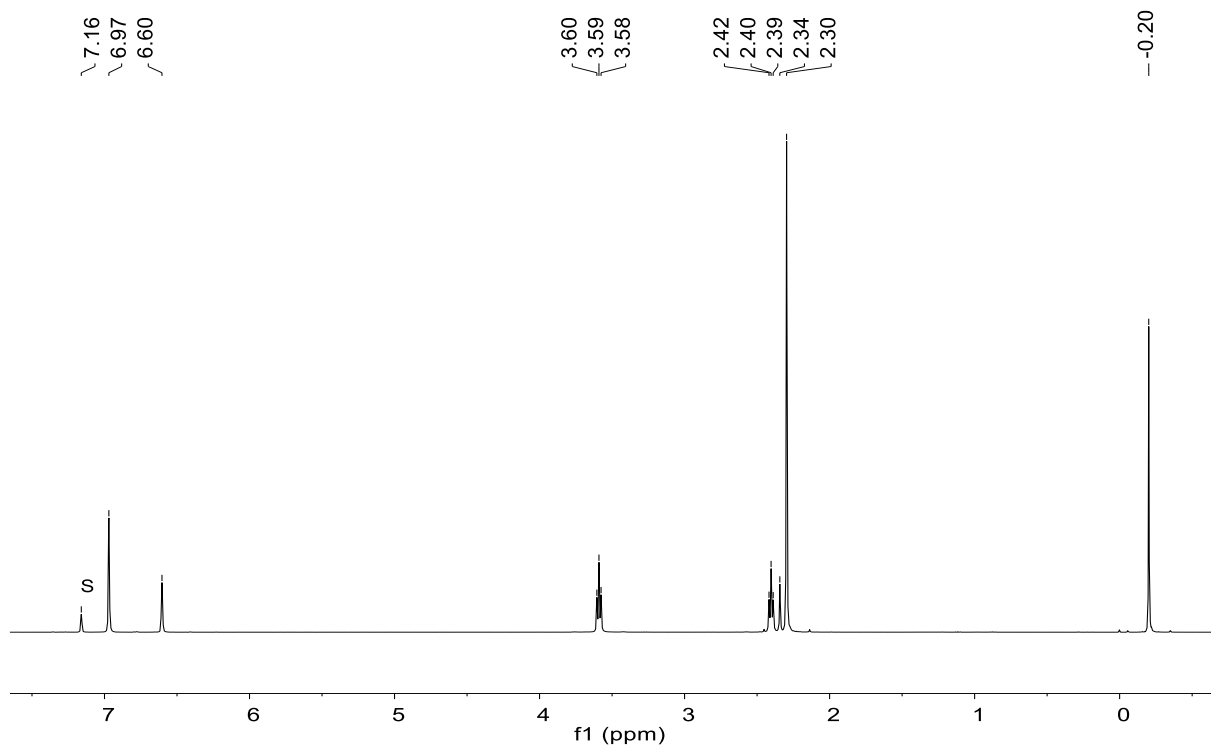
Figure S7. ^{1}H NMR spectrum of **1-CH$_2$SiMe$_3$** in benzene-d_6 at 296 K; S denotes the residual proton signal of the deuterated solvent.
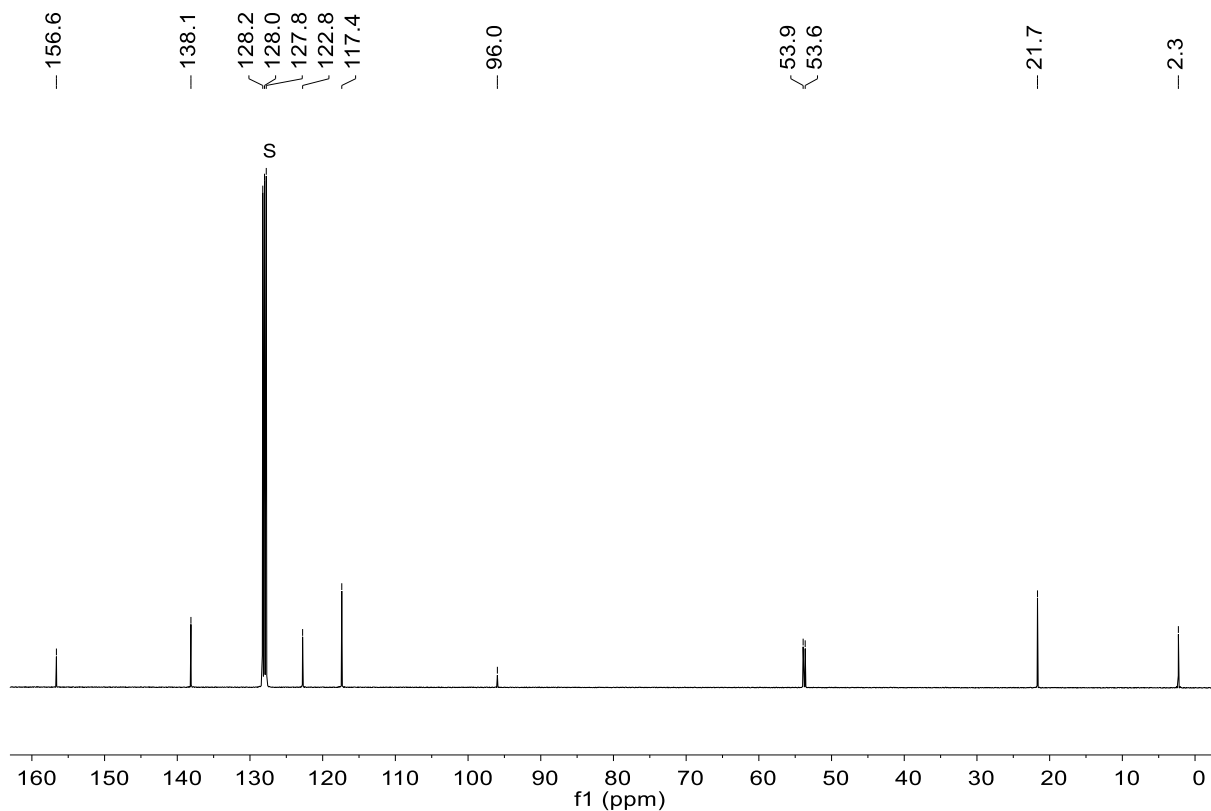
Figure S8. ^{13}C{^{1}H} NMR spectrum of **1-CH$_2$SiMe$_3$** in benzene-d_6 at 296 K; S denotes the residual proton signal of the deuterated solvent.
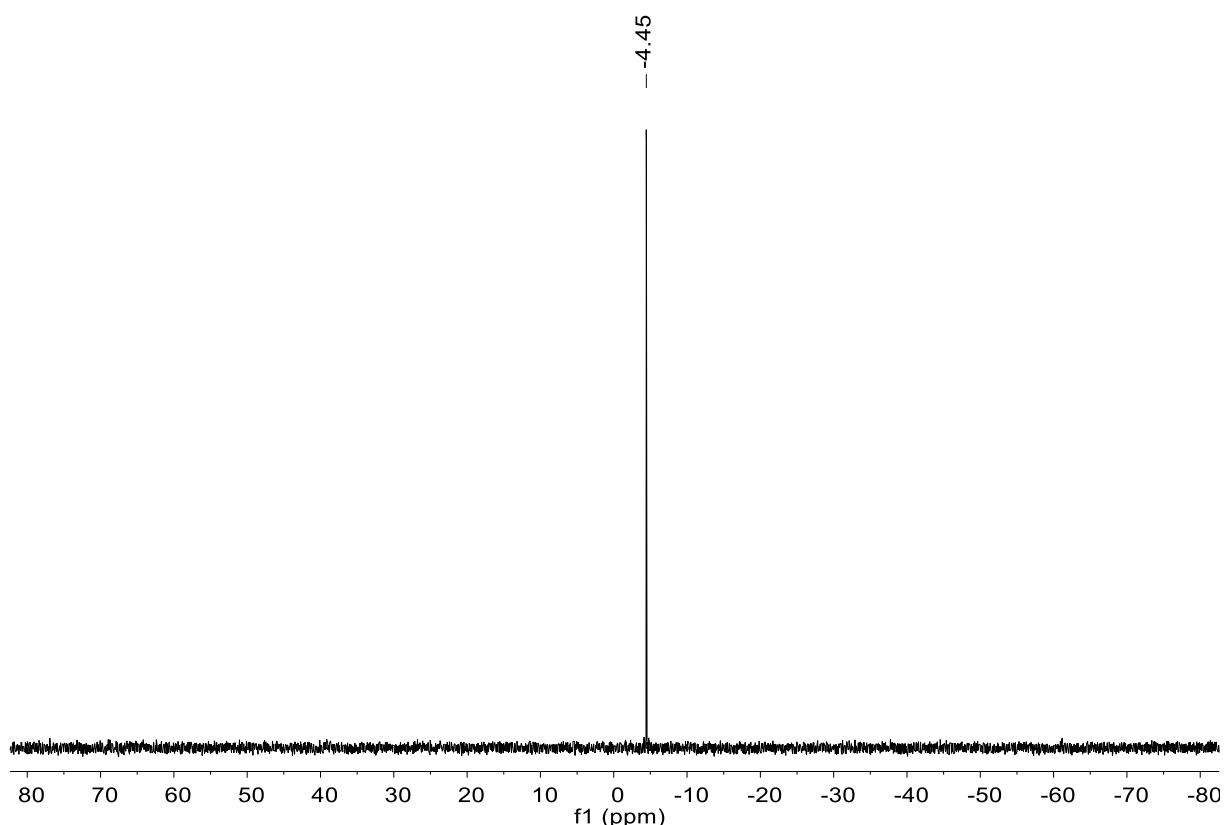
Figure S9. $^{29}Si\{^{1}H\}$ NMR spectrum of **1-CH₂SiMe₃** in benzene-d_6 at 296 K.

2.5. [Ti (Xy-N₃N)]₂ (2)

Route 1: A red solution of **1-Me** (70 mg, 0.135 mmol) in benzene (10 mL) was degassed and charged with 1 bar of dihydrogen gas. Upon heating the reaction mixture for 48 h at 60 °C, dark red crystals of **2** precipitated from the solution. The crystals were collected by decantation of the supernatant and washing with 10 mL of benzene at ambient temperature, and dried under reduced pressure; yield: 51 mg (0.101 mmol, 75%). Elemental analysis calcd. (%) for $C_{60}H_{78}N_8Ti_2$ (1007.07 g/mol): C 71.56, H 7.81, N 11.13%. Found: C 71.51, H 7.74, N 11.18%.

Route 2: **1-Me** (10 mg, 19 μmol) and PhSiH₃ (2.4 μL, 19 μmol) were mixed in a J. Young NMR tube. To this mixture was added 0.5 mL of benzene-d_6 at ambient temperature. The resulting bright red solution was heated at 60 °C for 18 h, upon which red crystals of **2** precipitated from the reaction mixture. Identity of the crystals was confirmed by IR spectroscopy.

Route 3: **1-CH₂SiMe₃** (10 mg, 17 μmol) was dissolved in 0.5 ml of benzene-d_6 and transferred into a J. Young NMR tube. The solution was degassed once and then pressurized with 1 bar of dihydrogen gas. The reaction mixture was heated to 80 °C for 5 days, resulting in the precipitation of the red crystals of **2**. Identity of the crystals were confirmed by IR spectroscopy.

Route 4: **1-CH₂SiMe₃** (20 mg, 34 μmol) and PhSiH₃ (4.2 μL, 34 μmol) were dissolved in 0.5 mL of benzene-d_6 and transferred into a J. Young NMR tube. The solution was heated at 80

°C for 5 days and the progress of the reaction was followed by ^{1}H NMR spectroscopy. Upon heating, red crystals of **2** precipitated from the reaction mixture. IR spectrum of the red crystals showed the IR bands of compound **2**.

Route 5: A mixture of **1-Cl** (100 mg, 0.186 mmol) and K (8 mg, 0.20 mmol, 1,1 equiv.) was treated with 10 mL of benzene at ambient temperature under N_2 atmosphere and stirred for 5 days. Upon stirring, the color of the solution changed from brown to light yellow with concomitant formation of a red precipitate. An aliquot NMR of the light yellow supernatant shows formation of $H_3(N_3N)$ as a by-product. Filtration of the supernatant and washing with benzene (5 mL) at ambient temperature afforded a red powder, which was dried for 3 h under reduced pressure to obtain compound **2** as a red solid. Yield: 58 mg (0.058 mmol, 62%).

IR (KBr pellet, RT, cm^{-1}): 2908 (m), 2868 (m), 2834 (m), 2804 (m), 1581 (vs), 1464 (m), 1443 (m), 1334 (s), 1322 (s), 1288 (m), 1192 (s), 1160 (m), 1142 (m), 1129 (m), 1111 (m), 1088 (w), 1076 (m), 1041 (m), 987 (m), 959 (m), 938 (m), 890 (m), 854 (w), 844 8w), 822 (s), 809 (s), 763 8w), 721 (m), 702 (m), 694 (m), 655 (m), 595 (s), 577 (w), 537 (m), 515 (w), 467 (m).
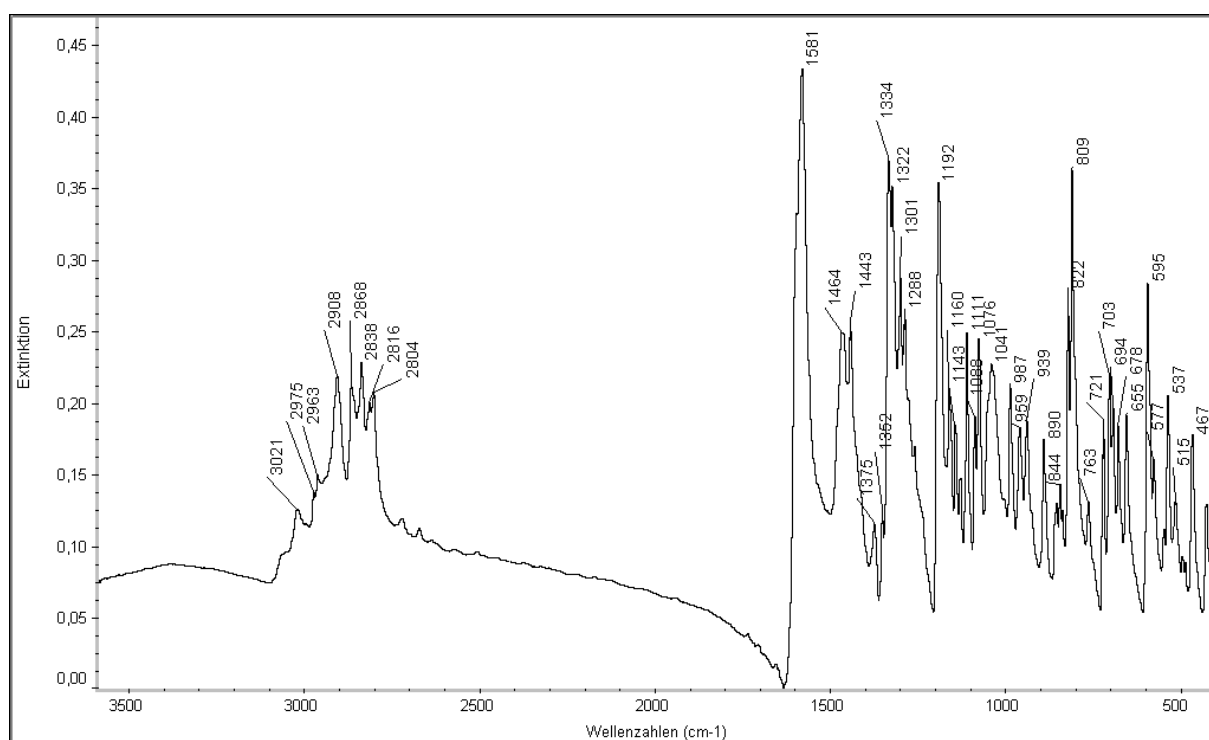
Figure S10: Solid state IR spectrum of **2** collected on KBr pellet at room temperature.

SQUID magnetometry evaluation of compound 2:

Magnetic data of compound **2** were recorded with a Quantum Design MPMS-5XL SQUID magnetometer. The polycrystalline sample was compacted and immobilized into a cylindrical PTFE capsule. The data were acquired as a function of the magnetic field (0.1−5.0 T at 2.0 K) and temperature (2.0–290 K at 0.1 T, 1.0 T, 3.0 T, and 5.0 T) and corrected for the diamagnetic contributions of the sample holder and the compound (χ_{dia} = −5.19×10^{-4} cm^3 mol^{-1}). Figure S11 shows the temperature dependent magnetic data of **2** as $\chi_m T$ vs T plot. Non-negligible divergences of the $\chi_m T$ values for T > 150 K at different magnetic fields indicate a very small content of ferri- or ferromagnetic impurities in the sample that probably was introduced during the sample preparation procedure. As the magnetization is not saturated, field-dependent measurements of the molar magnetic susceptibility allow to correct for this impurity at temperatures above 20 K, and at all fields up to 5 T.[S5]
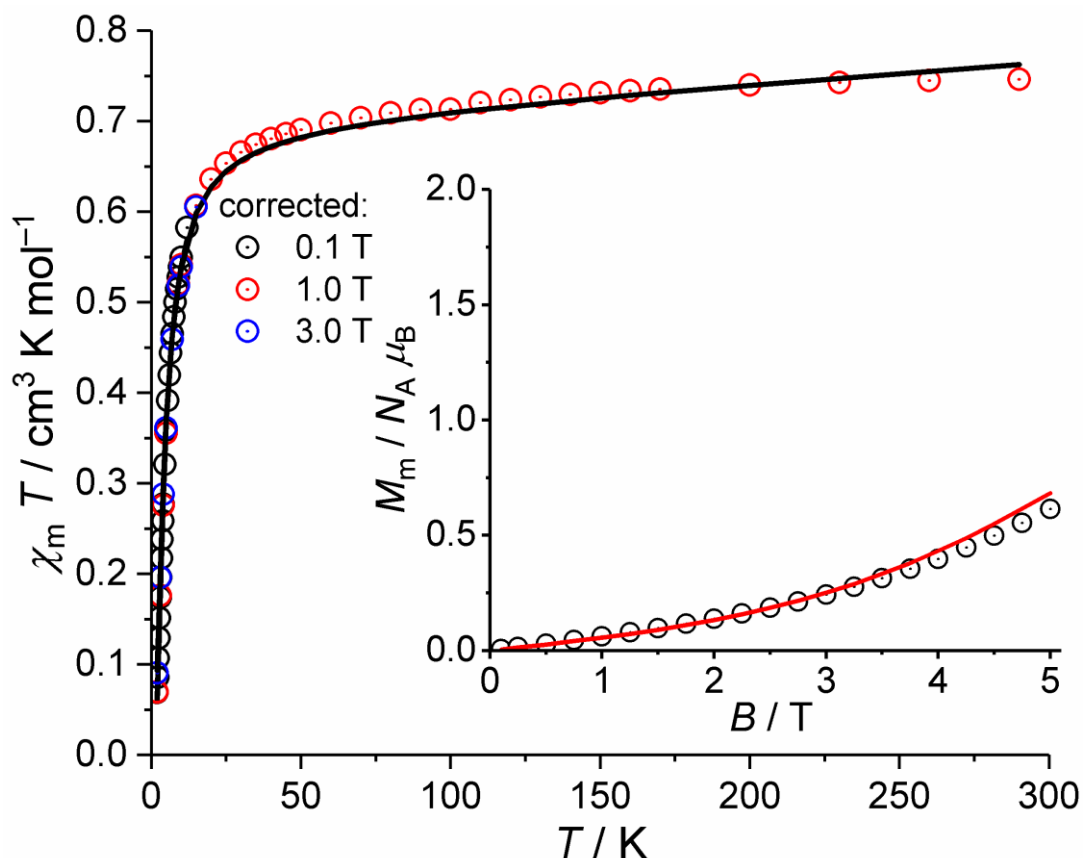
Figure S11: Temperature dependence of $\chi_m T$ for complex **2**, corrected for ferri-/ferromagnetic contaminations. Inset: Magnetization curve M_m *vs.* B at 2.0 K (circles: experimental data, lines: fit according to KQ-method). Solid lines represent the least-squares fit to an exchange-coupled Ti(III) dimer using CONDON 3.0.

Table S1. Simulated magnetic characteristics of **2** (*SQ*: relative root mean square error) established from a least-squares fit to the combined data shown in Figure S11. The exchange interaction energy *J* is calculated according to the Heisernberg-Dirac-van Vleck Hamiltonian in '$-2J\,S_1{\cdot}S_2$' convention. The two Ti(III) centers are assumed to adopt identical, C_{4v}-symmetric ligand environments, with ligand field parameters $B_k{}^q$ in Wybourne notation. All values except *SQ* are given in cm^{-1}.

ζ_{3d} [S6]	154
$B^2{}_0$	-17831 ± 37
$B^4{}_0$	-9086 ± 100
$B^4{}_4$	30979 ± 29
J	-2.6 ± 0.1
SQ	2.2 %

2.6. $K_2[\{(Xy\text{-}N_3N)Ti\}_2(\mu_2\text{-}N_2)]$ (3)

Route 1: A Schlenk flask containing potassium mirror (92 mg, 2.35 mmol, 2,5 equiv.) was charged with **1-Cl** (500 mg, 0.93 mmol) and the mixture treated with ~30 mL of pre-cooled THF at -80 °C under N_2 atmosphere. The resulting dark brown mixture was stirred for 48 h at ambient temperature and the progress of the reaction was followed by ^{1}H NMR spectroscopy. Upon stirring the color of the solution changed to red-brown. All volatiles were removed after completion of the reaction and the dark red-brown residue was extracted with benzene (2 × 20 mL). The red extracts were concentrated to ~5 mL and to the red suspension were added ~20 mL of *n*-pentane. The red precipitate was isolated by filtration from the light red supernatant and washing with 10 mL of *n*-pentane at ambient temperature. The solid was dried under reduced pressure for 3 h at room temperature to give the product as analytically pure, air-sensitive, red solid; yield: 318 mg (0.29 mmol, 61%). Elemental analysis calcd. (%) for $C_{60}H_{78}K_2N_{10}Ti_2$ (1113.26 g/mol): C 64.73, H 7.06, N 12.58%. found: C 63.47, H 7.09, N 9.97%.

Route 2: A dark brown solution of **1-Cl** (500 mg, 0.93 mmol) in 20 mL of THF was treated with a THF solution of potassium naphthalenide (15 mL, 0.133 mol/L, 1.99 mmol, 2.15 equiv.) at -78 °C under N_2 atmosphere. Immediate after addition, the color of the solution chnaged to reddish brown. Resulting solution was slowly brought to room temperature over 2 h. An aliquot NMR confirmed the complete and selective conversion of the starting materials into the products. The reddish brown solution was concentrated to ~20 mL and treated with 3 mL of *n*-pentane. The suspension was filtered and the filtrate was evaporated to dryness. The residue was washed with *n*-hexane (3 × 10 mL) and a 3:1 *n*-hexane/benzene mixture (8 mL) to obtain a spectroscopically pure reddish brown solid; yield: 446 mg (0.40 mmol, 86%).

^{1}H NMR (400 MHz, THF-d_8, 296 K): δ (ppm) = 1.89 (s, 36H, $C_6H_3(CH_3)_2$), 2.76 (t, ^3J(H,H) = 5.9 Hz, 12H, NCH_2), 3.41 (t, ^3J(H;H) = 5.9 Hz, 12H, NCH_2), 5.83 (br. s, 6H, *p*-C_6H_3), 7.23 (br. s, 12H, *o*-C_6H_3).

$^{13}C\{^1H\}$ NMR (101 MHz, THF-d_8, 296 K): δ (ppm) = 21.5 (s, C$_6$H$_3$(CH$_3$)$_2$), 49.6 (s, NCH$_2$), 52.8 (s, NCH$_2$), 116.7 (s, o-C$_6$H$_3$), 117.3 (s, p-C$_6$H$_3$), 137.5 (s, m-C$_6$H$_3$), 161.8 (s, $ipso$-C$_6$H$_3$).

IR (KBr pellet, RT, cm^{-1}): 3018 (w), 2945 (m), 2912 (m), 2846 (s), 1579 (vs), 1468 (s), 1376 (w), 1320 (s), 1298 (s), 1186 (s), 1144 (m), 1088 (m), 1036 (m), 987 (m), 962 (w), 878 (w), 817 (m), 789 (vw), 754 (w), 692 (s), 593 (w), 549 (w), 516 (w), 491 (w).
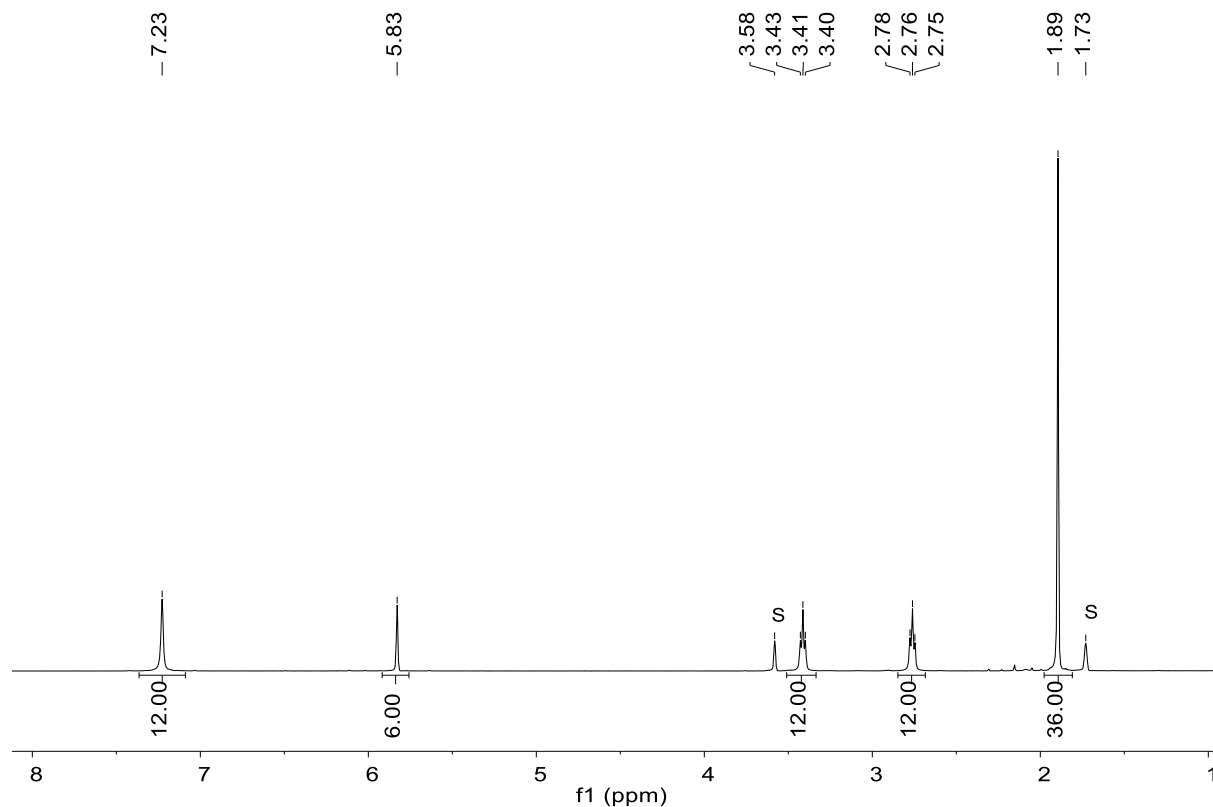
Figure S12. ^{1}H NMR spectrum of **3** in THF-d_8 at 296 K; S denotes the residual proton signal of the deuterated solvent.
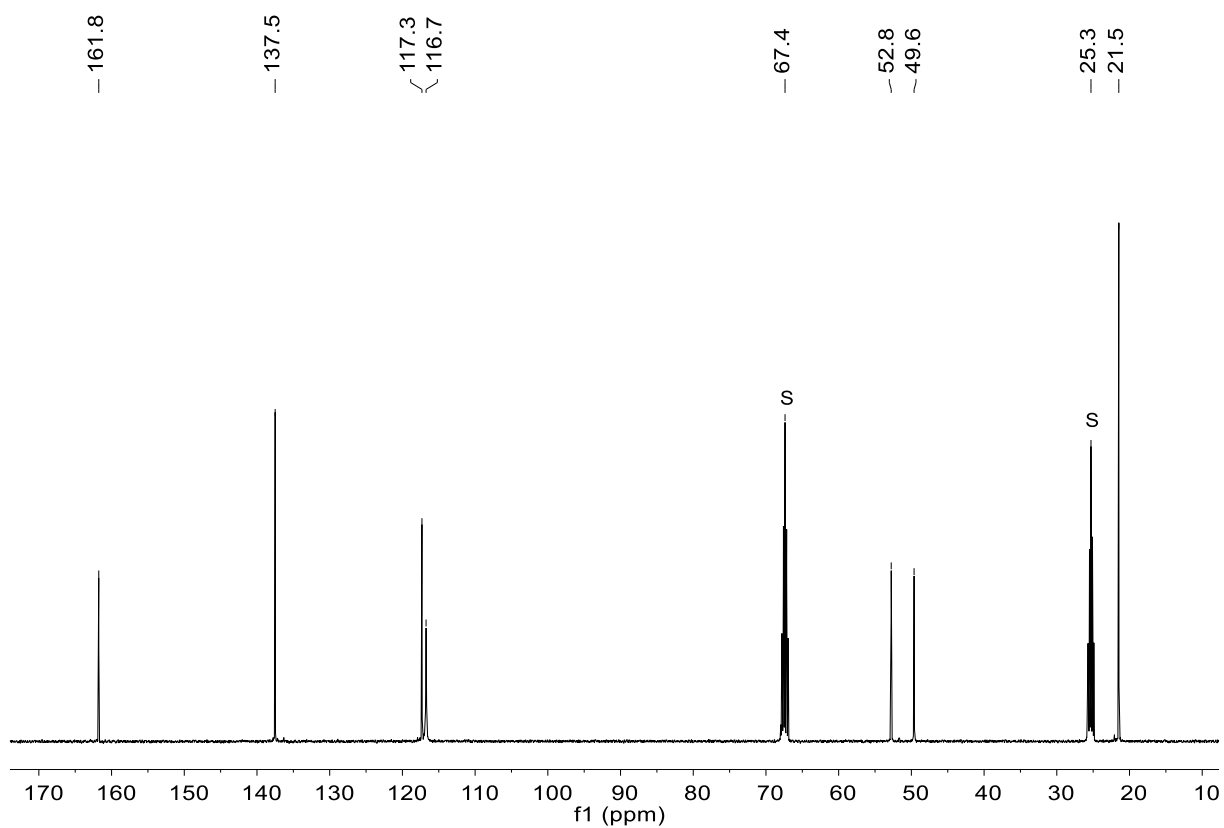
Figure S13. ^{13}C{^{1}H} NMR spectrum of **3** in THF-d_8 at 296 K; S denotes the residual proton signal of the deuterated solvent.
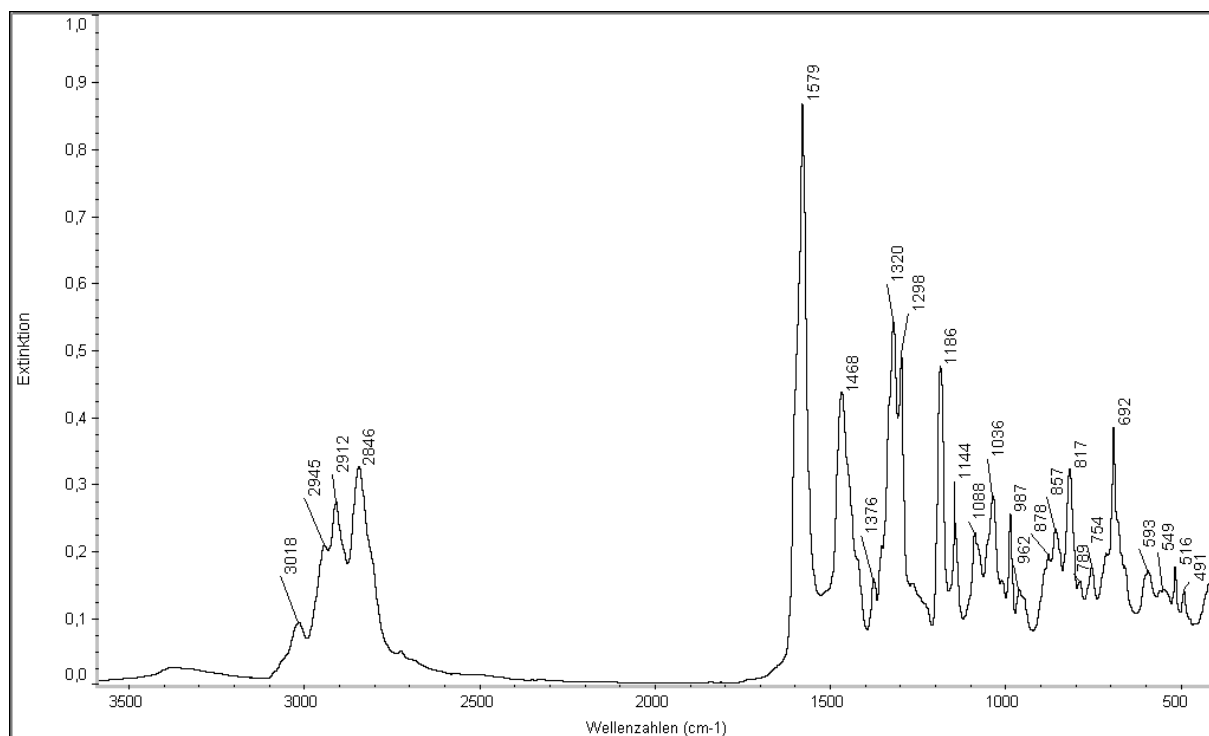
Figure S14: Solid state IR spectrum of **3** collected on KBr pellet at room temperature.

2.7. $K_2[\{(Xy\text{-}N_3N)Ti\}_2(\mu_2\text{-}^{15}N_2)]$ $(3\text{-}^{15}N_2)$

A Schlenk tube was charged with **1-Cl** (100 mg, 0.19 mmol), K (16 mg, 0.41 mmol, 2.2 equiv.) and naphthalene (52 mg, 0.41 equiv., 2.2 equiv.), and to this solid mixture pre-cold (−78°C) THF was added under $^{15}N_2$ gas. The brown solution was stirred at room temperature over 3 h. Upon stirring the color of the solution changed to red brown. The solution was treated with 1 mL of *n*-pentane, filtered and the reddish brown filtrate was evaporated to dryness. The residue was washed with *n*-pentane (2 × 3 mL) and dried under reduced pressure at ambient temperature for 2 h to afford **3-$^{15}N_2$** as a red brown solid; yield: 86 mg (0.08 mmol, 83%).

^{15}N NMR (40.57 MHz, THF-d_8, 296 K): δ (ppm) = 393.9 ppm. All other NMR data are identical to **3**.
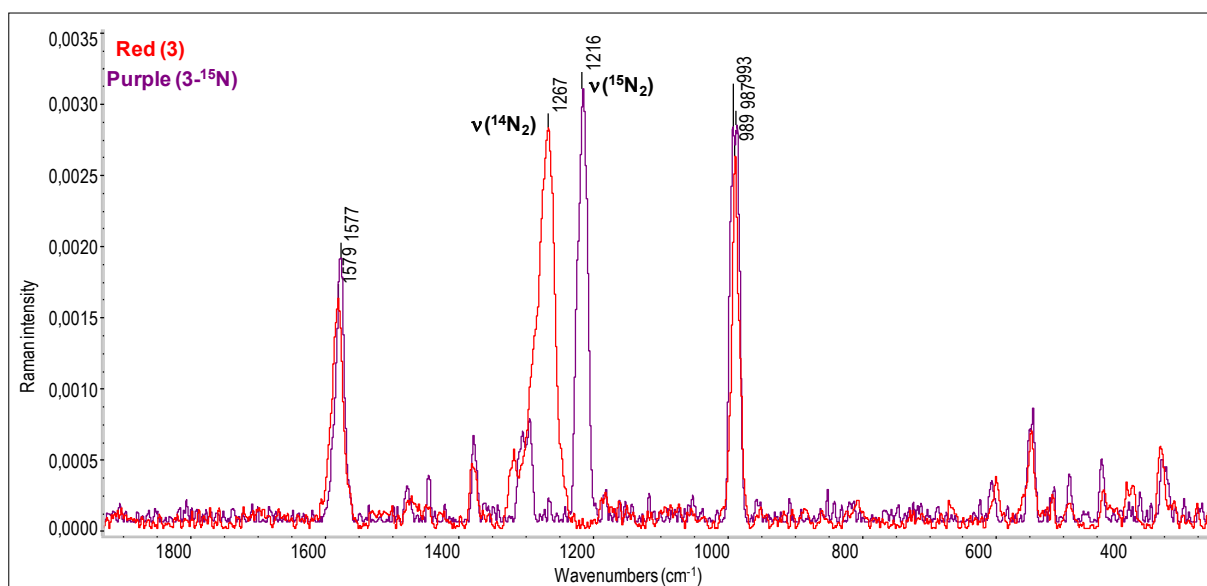
Figure S15: Solid state Raman spectra of **3** and **3-^{15}N** collected at room temperature.
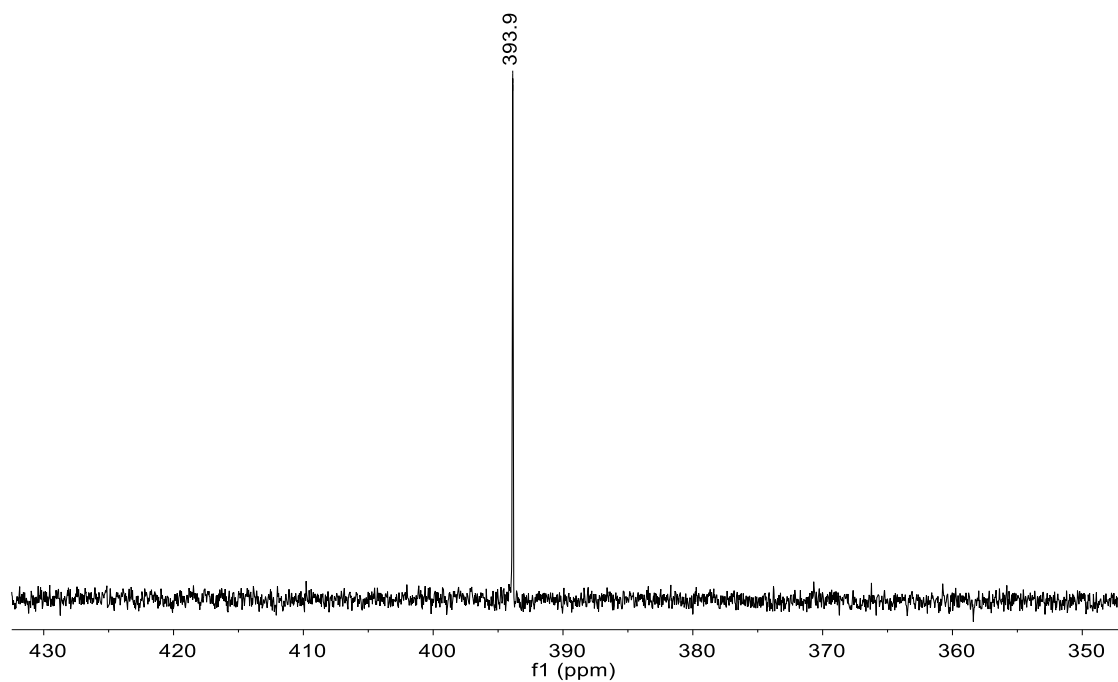
Figure S16. ^{15}N NMR spectrum of **3-^{15}N** in THF-d_8 at 296 K.

3. Catalytic conversion of N$_2$ to N(SiMe$_3$)$_3$ using 3 as a catalyst

A Schlenk bomb fitted with Teflon valve was charged with **3** (10 mg, 0.009 mmol), Me$_3$SiCl (1.464 g, 13.5 mmol, 1500 equiv.), K (526 mg, 13.5 mmol, 1500 equiv.), 1.5 mL of THF-d_8 containing cyclohexane as reference and N$_2$ gas (~1 bar), and stirred at ambient temperature. Progress of the conversion was followed by ^{1}H NMR and the quantification of formed N(SiMe$_3$)$_3$ was done at a 24 h interval by comparing with cyclohexane reference. To confirm the accuracy of the NMR method for the quantification of N(SiMe$_3$)$_3$, selected samples were also checked by GC-MS. The results of the GC-MS method fit well with that of the NMR method.

Reaction with Li-metal, Na-sands, K with catalytic amount of naphthalene and KC$_8$ was also carried out following the same procedure.

Table S2: Catalytic silylation of N$_2$ with**1-Cl**, **1-Me**, **2** and **3** as catalyst in THF-d_8 at room temperature.

Entry	Catalyst	Reductant	Me$_3$SiCl/reductant (eq.)	Time	N(SiMe$_3$)$_3$/Ti (eq.)	e$^-$ yield (%)
1	**1-Cl**	K	200/200	7d	2	6
2	**1-Me**	K	150/150	7d	2	8
3	**2**	K	1500/1500	7d	3.9	1,6
4	**3**	Li	1500/1500	7d	7	2.8
				16d	17	6.8
5	**3**	Na	1500/1500	7d	3,5	1.4
6	**3**	K	1500/1500	1d	4,5	1.8
				2d	7,5	3.0
				3d	9	3.6
				5d	13,5	5.4
				7d	16,5	6.6
7	**3**	KC$_8$	1500/1500	7d	~0,5	-
8	**3**	K + C$_{10}$H$_8$ (cat.)	1500/1500	7d	9,5	3.8

In all catalytic runs a significant amount of Me$_3$Si-SiMe$_3$ and a small amount of Me$_3$SiH has also formed, presumably by combination of Me$_3$Si radical and abstraction of hydrogen by Me$_3$Si radical, respectively.
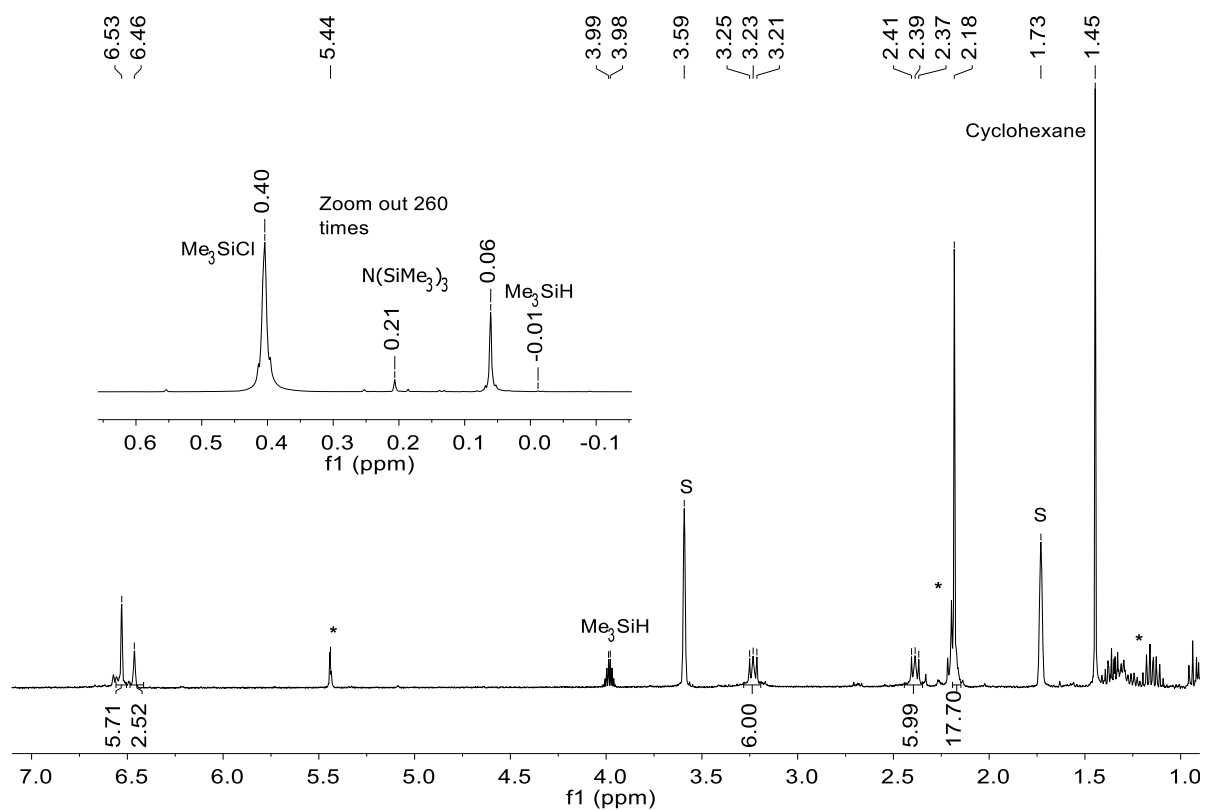
Figure S17. ^{1}H NMR spectrum of the crude reaction mixture during catalysis with Li metal after 7 days in THF-d_8 at 296 K; S denotes the residual proton signal of the deuterated solvent and * denotes some unknown by-product.
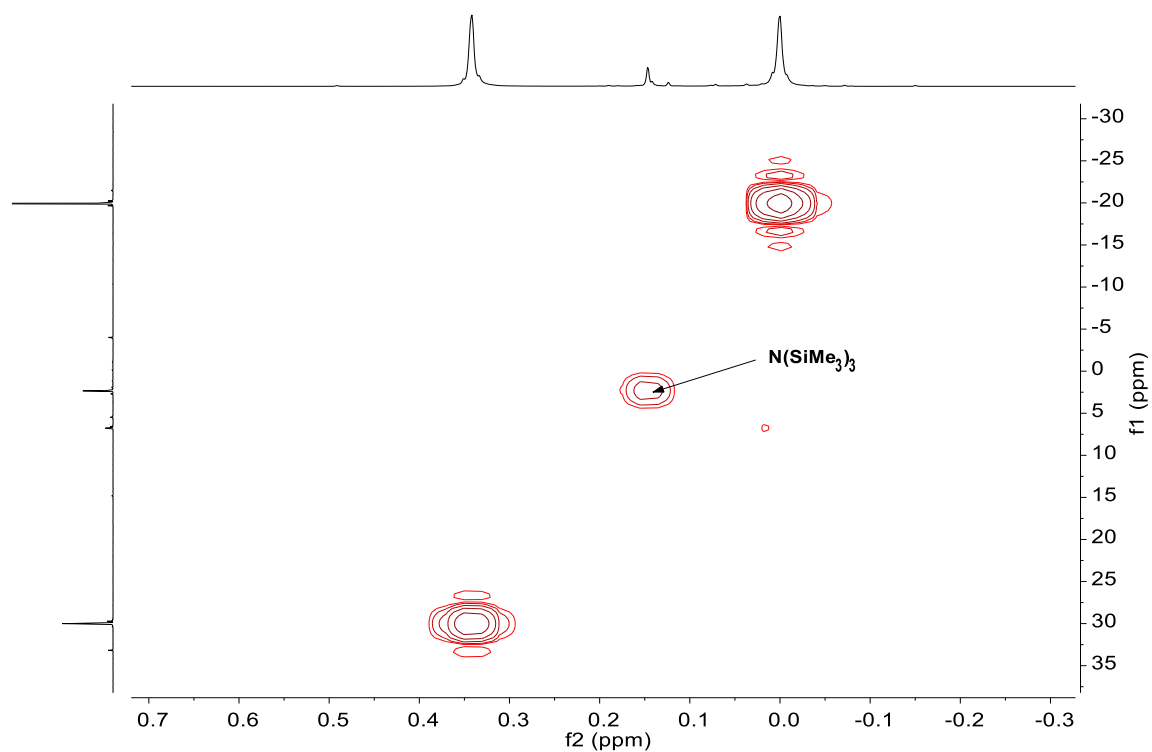
Figure S18. ^{1}H-^{29}Si HMBC correlation spectrum of a catalysis mixture in THF-d_8 at 296 K.
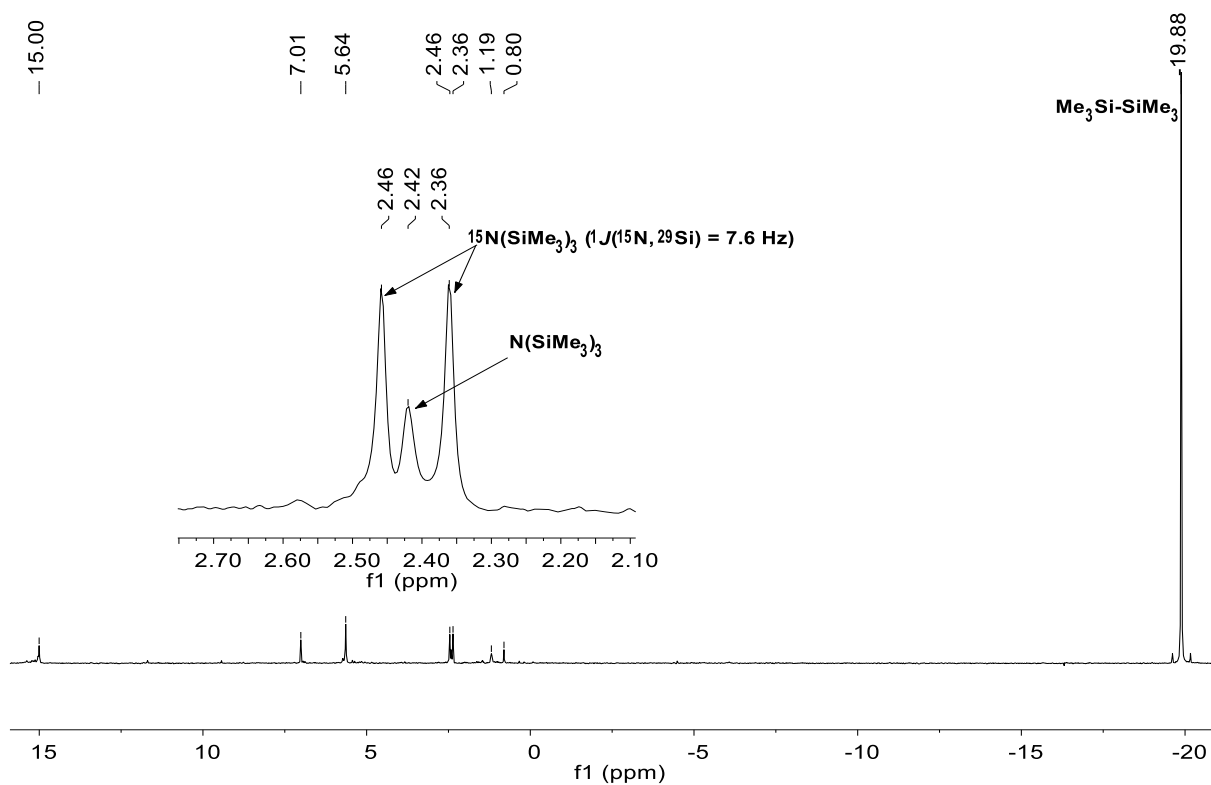
Figure S19. $^{29}Si\{^1H\}$ NMR spectrum of the crude reaction mixture during catalysis with **3** as a catalyst, K as a reducing agent and $^{15}N_2$ as nitrogen source after 2 days in THF-d_8 at 296 K.
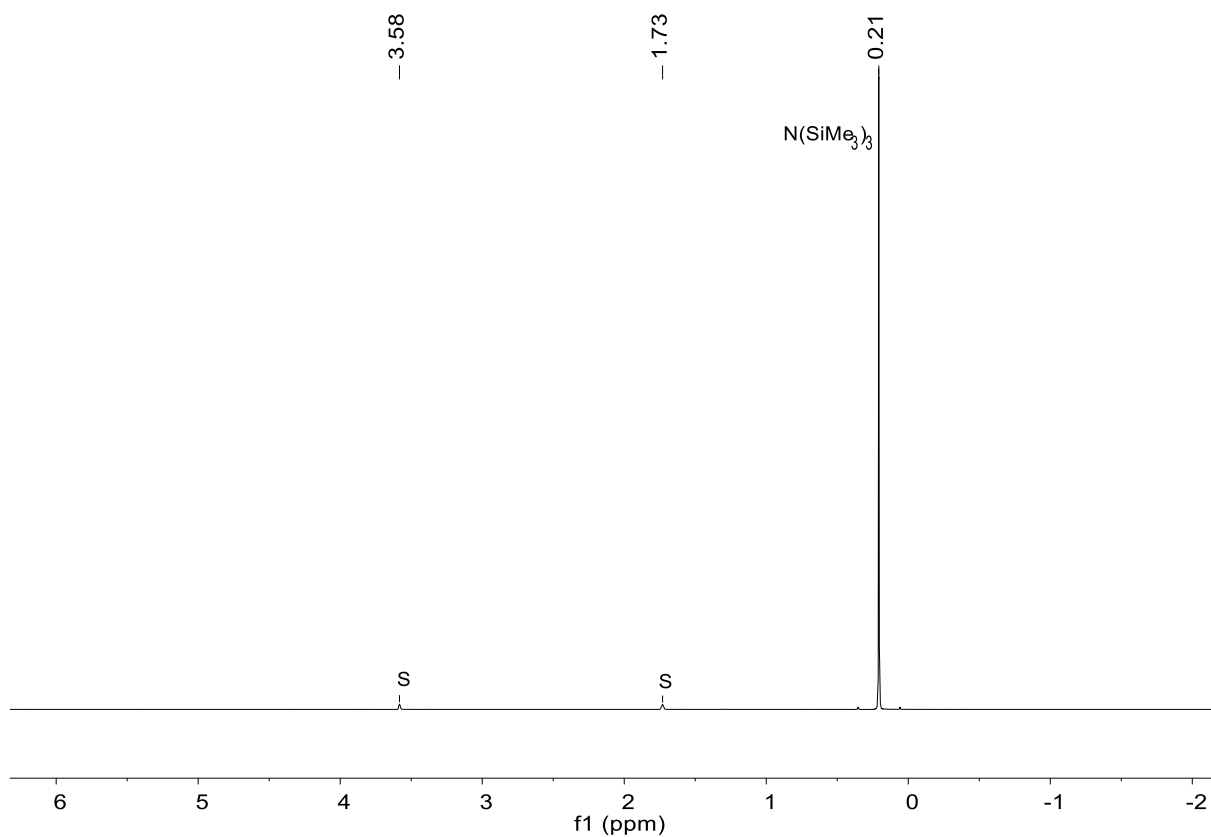
Figure S20. ^1H NMR spectrum of pure $N(SiMe_3)_3$, prepared independently from the reaction of Me_3SiCl and $KN(SiMe_3)_2$, in THF-d_8 at 296 K; S denotes the residual proton signal of the deuterated solvent.
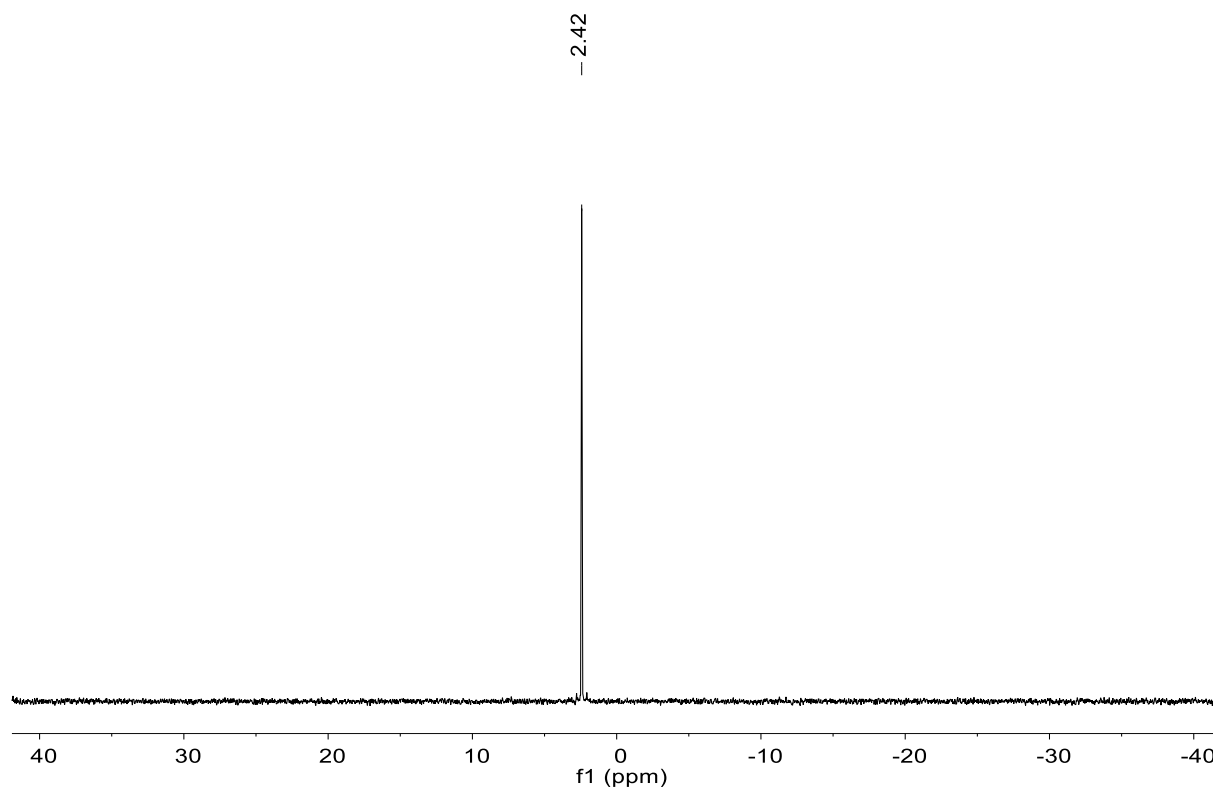
Figure S21. $^{29}Si\{^1H\}$ NMR spectrum of pure $N(SiMe_3)_3$, prepared independently from the reaction of Me_3SiCl and $KN(SIMe_3)_2$, in THF-d_8 at 296 K.

NMR spectroscopic data of [Ti(N(SiMe₃)₂)(Xy-N₃N)]:

For NMR of **[Ti(N(SiMe₃)₂)(Xy-N₃N)]**, catalysis was carried out with 200 mg (0.180 mmol) of **3**, 1,952 g (18 mmol, 100 equiv.) of Me_3SiCl and 700 mg (18 mmol, 100 equiv.) of K in 10 mL of THF at ambient temperature. After 7 days all volatiles were removed under reduced pressure and a part of the residue was extracted with 0.5 mL of C_6D_6 for NMR spectroscopic measurement.

^1H NMR (400 MHz, benzene-d_6, 296 K): δ (ppm) = 0.21 (s, 18H, $N(Si(CH_3)^3)_2$), 2.19 (s, 18H, $C_6H_3(CH_3)_2$), 2.53 (t, $^3J(H,H)$ = 7.4 Hz, 6H, NCH_2), 3.37 (t, $^3J(H,H)$ = 7.4 Hz, 6H, NCH_2), 6.52 (s, 3H, p-C_6H_3), 6.71 (s, 6H, o-C_6H_3).

$^{13}C\{^1H\}$ NMR (101 MHz, benzene-d_6, 296 K): δ (ppm) = 1.1 (s, $N(Si(CH_3))_2$), 21.7 (s, $C_6H_3(CH_3)_2$), 47.7 (s, NCH_2), 56.1 (s, NCH_2), 120.9 (s, o-C_6H_3), 123.1 (s, p-C_6H_3), 138.2 (s, m-C_6H_3), 149.3 (s, $ipso$-C_6H_3).

$^{29}Si\{^1H\}$ NMR (79.5 MHz, benzene-d_6, 296 K): δ (ppm) = 5.58 ppm
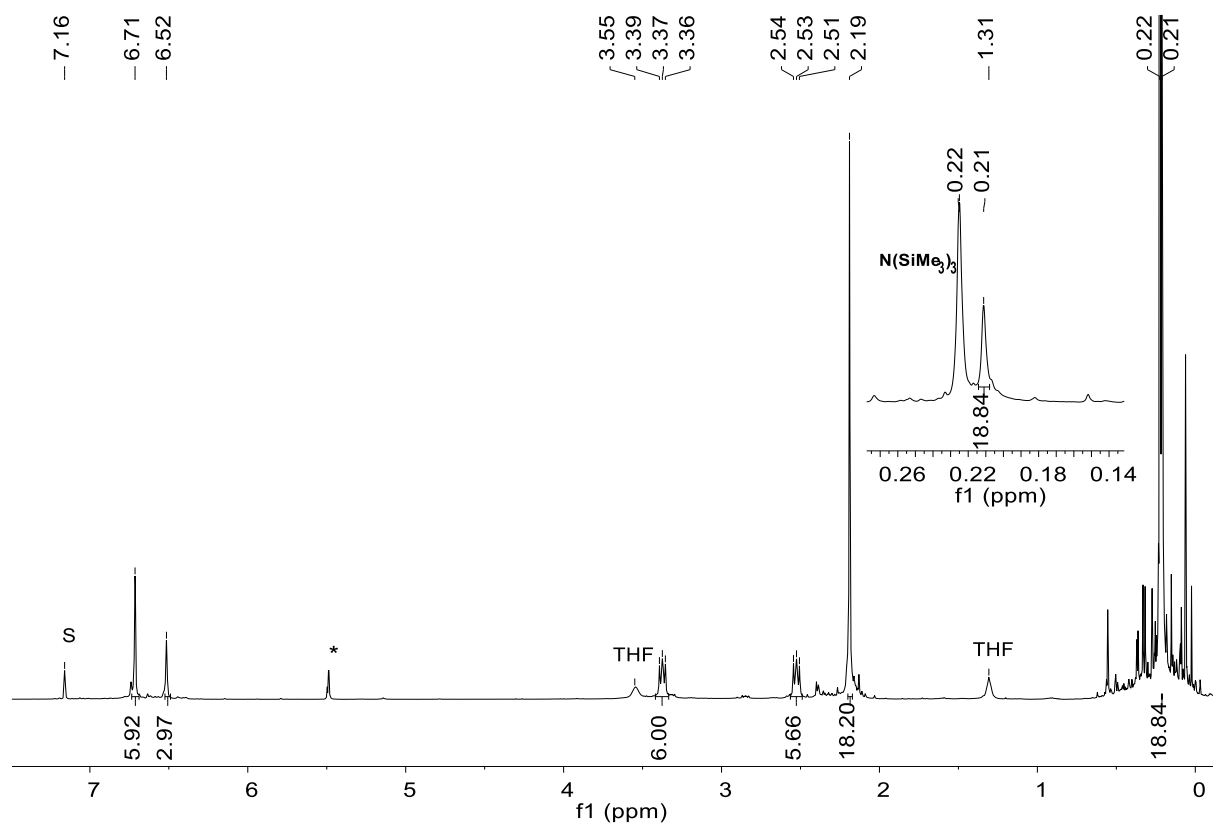
Figure S22. ¹H NMR spectrum of **[Ti(N(SiMe₃)₃(Xy-N₃N)]** in benzene-*d*₆ at 296 K; S denotes the residual proton signal of the deuterated solvent; * corresponds to some unknown signal.
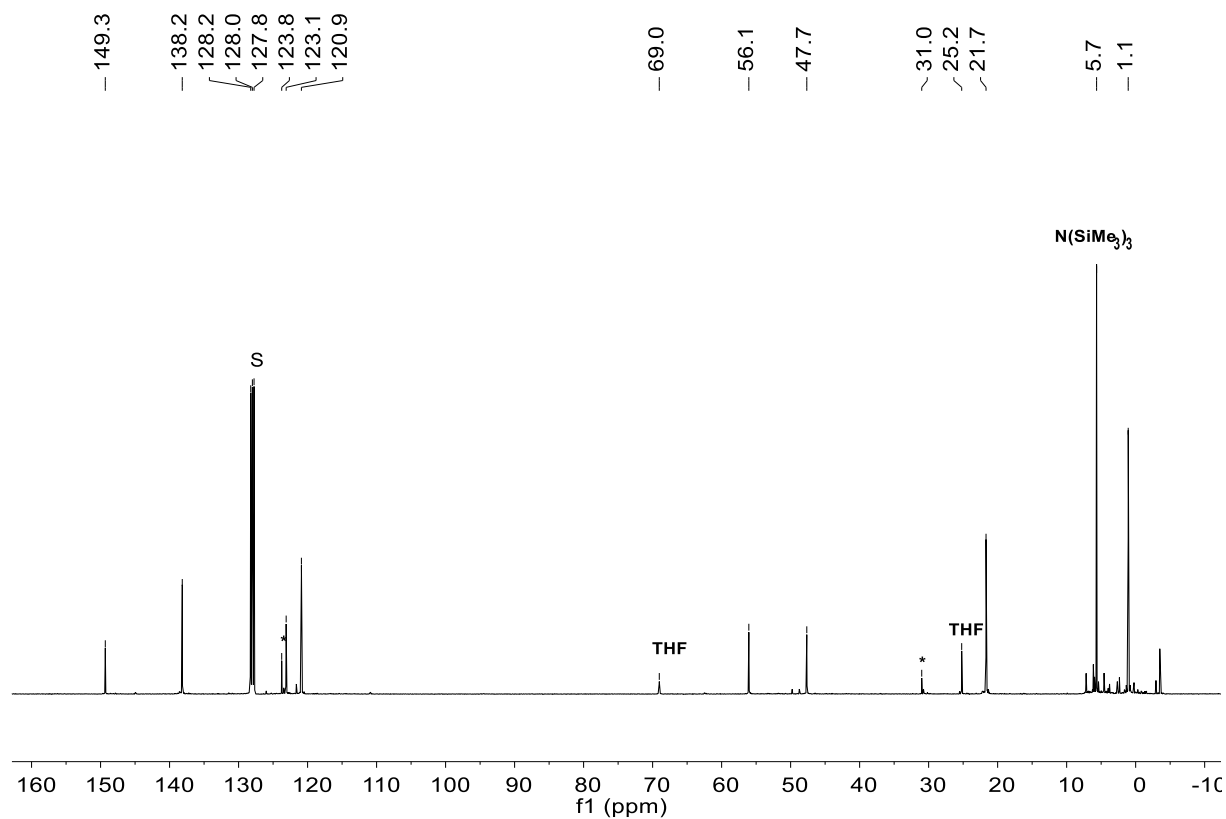
Figure S23. ¹³C{¹H} NMR spectrum of **[Ti(N(SiMe₃)₃(Xy-N₃N)]** in benzene-*d*₆ at 296 K; S denotes the residual proton signal of the deuterated solvent; * corresponds to some unknown signal.
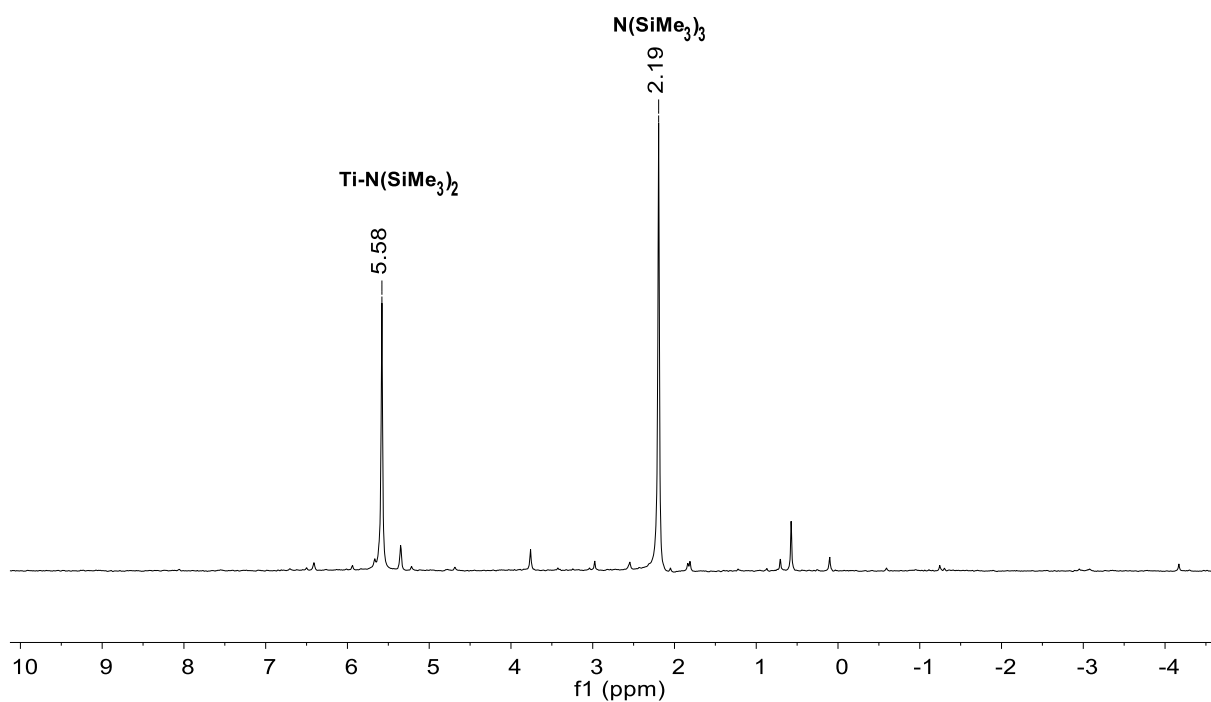
Figure S24. $^{29}Si\{^1H\}$ NMR spectrum of **[Ti(N(SiMe₃)₃(Xy-N₃N)]** in benzene-d_6 at 296 K.
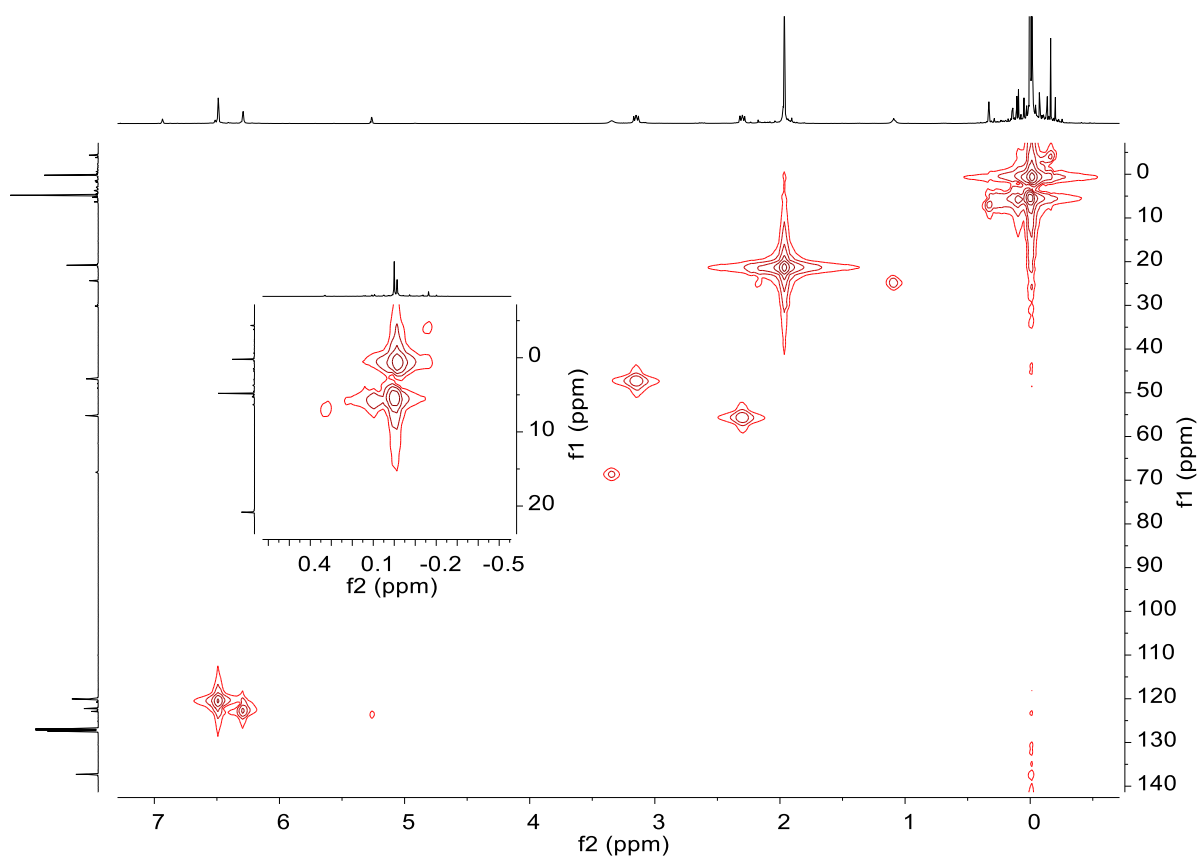
Figure S25. ^1H-^{13}C HMQC correlation NMR spectrum of **[Ti(N(SiMe₃)₃(Xy-N₃N)]** in benzene-d_6 at 296 K.
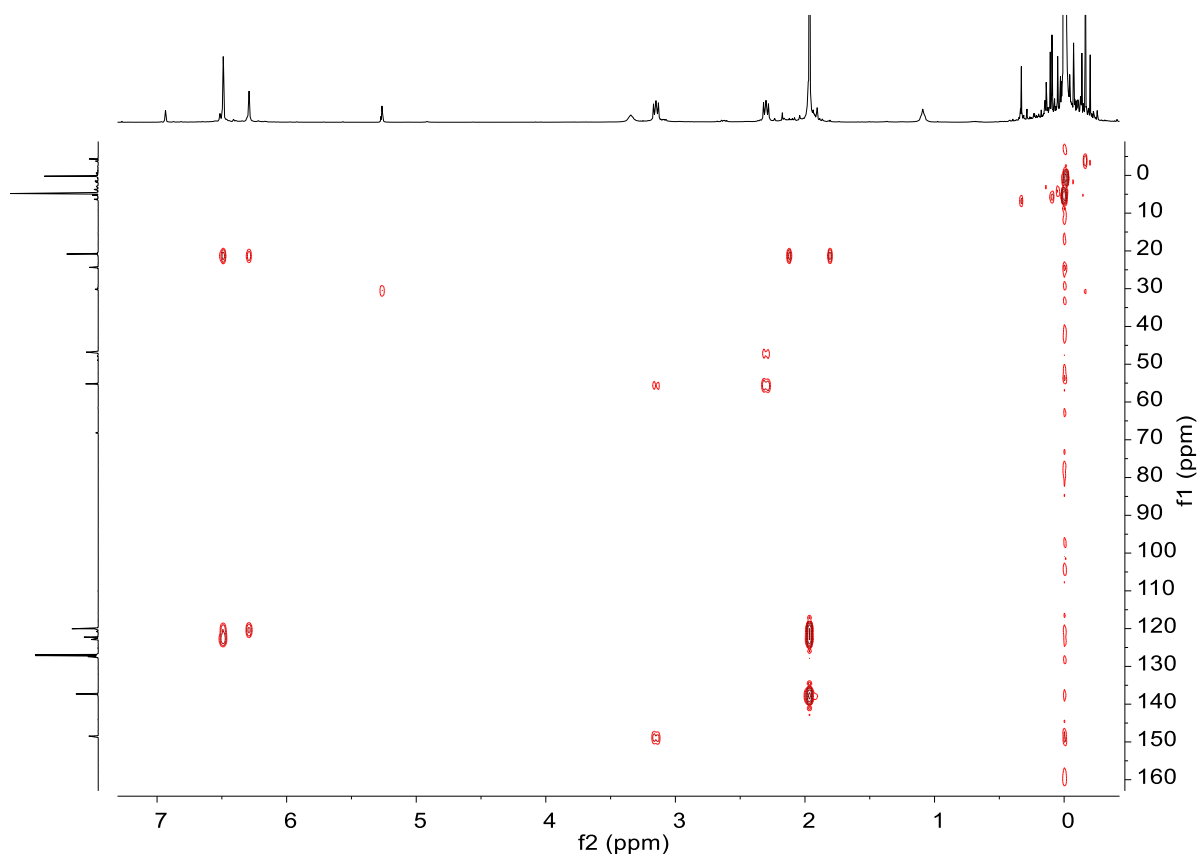
Figure S26. ^{1}H-^{13}C HMBC correlation NMR spectrum of **[Ti(N(SiMe₃)₃(Xy-N₃N)]** in benzene-d_6 at 296 K.

4. Crystal structure determination of compounds 2 and 3

X-ray diffraction data were collected on a Bruker D8 goniometer with an APEX CCD area-detector (**2**) or on an Eulerian 4-circle diffractometer STOE STADIVARI (**3**) in ω-scan mode with Mo-Kα radiation (λ = 0.71073 Å). Measurements were carried out at 100 K. The structures were solved by direct methods using SIR-97.[S7] All refinements were carried out against F^2 with SHELXL. [S8] as implemented in the program system Olex2.[S9] In the refinement of **2**, the reflection 1 0 0 was omitted, because it was probably affected by the beamstop. The structure of **3** was treated as a two component inversion twin with a relative batch scale factor (BASF) of 0.379. All non-hydrogen atoms were refined with anisotropic displacement parameters. The hydrogen atoms in **2** were refined in their position with isotropic displacement parameters. The hydrogen atoms in **3** were included in calculated positions and treated as riding throughout the refinement with isotropic refinement parameters of U_H = 1.5•U_C for the CH_3 units and with U_H = 1.2•U_C for the CH_2 and for the CH units. Refinement results are given in Table S3. Graphical representations were performed with the program DIAMOND.[S10] CCDC-1883119 (**2**) and CCDC-1883120 (**3**) contain the supplementary crystallographic data for this paper. These data can be obtained free of charge from the Crystallographic Data Centre via www.ccdc.cam.ac.uk/data_request/cif.

Table S3: Crystallographic data of **2** and **3**

	2	3
formula	$C_{60}H_{78}N_8Ti_2$	$C_{68}H_{94}N_{10}K_2O_2Ti_2$
Fw /g·mol^{-1}	1007.10	1257.53
cryst. color, habit	red block	orange block
crystal size / mm	0.21 × 0.19 × 19	0.56 × 0.473 × 0.35
crystal system	monoclinic	monoclinic
space group	*P2$_1$/c* (no. 14)	*P2$_1$* (no. 4)
a / Å	12.7525(10)	11.9665(4)
b / Å	14.9942(12)	13.9590(5)
c / Å	14.8095(11)	19.5766(6)
β / °	112.2429(11)	92.472(3)
V / Å^3	2621.1(4)	3267.04(19)
Z	2	2
d$_{calc}$/Mg·m^{-3}	1.276	1.278
μ(MoKα)/mm^{-1}	0.352	0.424
F(000)	1076.0	1340
θ range / °	2.03 - 24.93	2.03 - 25.35
index ranges	-17 ≤ h ≤ 17, -20 ≤ k ≤ 21, -20 ≤ l ≤ 20	-14 ≤ h ≤ 14, -16 ≤ k ≤ 16, -23 ≤ l ≤ 23
refln.	39213	87675
independ. reflns (*R*$_{int}$)	7498 (0.0378)	11954 (0.1103)
observed reflns	6476	8419
data/ restr./ param.	7498 / 0/ 472	11954 / 1 /770
R$_1$, *wR*2 [*I*> 2σ(*I*)]	0.0368, 0.0923	0.0544, 0.1181
R$_1$, *wR*2 (all data)	0.0439, 0.0973	0.0881, 0.1315
GooF on *F^2*	1.021	0.960
largest diff. peak, hole/ e·Å^3	0.47, -0.25	0.33, -0.29
CCDC number	1883119	1883120

5. References

S1. (a) G. E. Greco, A. I. Popa, R. R. Schrock, *Organometallics* **1998**, *17*, 5591; (b) G. E. Greco, R. R. Schrock, *Inorg. Chem*. **2001**, *40*, 3850.

S2. G. M. Diamond, R. F. Jordan, *Organometallics* **1996**, *15*, 4030.

S3. C. Tessier-Youngs, O. T. Beachley Jr., J. P. Oliver, K. Butcher, *Inorg. Synth.* **1986**, *24*, 95.

S4. (a) K. Fredenhagen, G. Cadenbach, *Z. Anorg. Allg. Chem*.**1926**, *158*, 249. (b) W. Rüdorff, E. Schulze, *Z. Anorg. Allg. Chem*.**1954**, *277*, 156.

S5. (a) K. Honda, *Annal. Phys.* **1910**, *337*, 1027; (b) F. Kohlrausch, *Praktische Physik*, Vol. 2, 23 ed., Teubner, Stuttgart, **1985**.

S6. J. S. Griffith, *The Theory of Transition-Metal Ions*, Cambridge University Press, Cambridge, **1980**.

S7. M. C. Burla, R. Caliandro, M. Camalli, B. Carrozzini, G. L. Cascarano, L. De Caro, C. Giacovazzo, G. Polidori, D. Siliqi, R. Spagna, *J. Appl. Crystallogr.* **2007**, *40*, 609-613.

S8. G. M. Sheldrick, *Acta Crystallogr. A* **2008**, *64*, 112-122.

S9. O. V. Dolomanov, L. J. Bourhis, R. J. Gildea, J. A. K. Howard, H. Puschmann, *J. Appl. Cryst.* **2009**, 42, 339-341.

S10. H. Putz, K. Brandenburg, *Diamond - Crystal and Molecular Structure Visualization*, *Crystal Impact*, Bonn, **2017**.